Ataxia with loss of Purkinje cells in a mouse model for Refsum disease

Sacha Ferdinandusse[a,1,2], Anna W. M. Zomer[b,1], Jasper C. Komen[a], Christina E. van den Brink[b], Melissa Thanos[a], Frank P. T. Hamers[c], Ronald J. A. Wanders[a,d], Paul T. van der Saag[b], Bwee Tien Poll-The[d], and Pedro Brites[a]

Academic Medical Center, Departments of [a]Clinical Chemistry (Laboratory of Genetic Metabolic Diseases) and [d]Pediatrics, Emma's Children Hospital, University of Amsterdam, 1105 AZ Amsterdam, The Netherlands; [b]Hubrecht Institute, Royal Netherlands Academy of Arts and Sciences 3584 CT Utrecht, The Netherlands; and [c]Rehabilitation Hospital ''De Hoogstraat'' Rudolf Magnus Institute of Neuroscience, 3584 CG Utrecht, The Netherlands

Edited by P. Borst, The Netherlands Cancer Institute, Amsterdam, The Netherlands, and approved October 3, 2008 (received for review June 23, 2008)

Refsum disease is caused by a deficiency of phytanoyl-CoA hydroxylase (PHYH), the first enzyme of the peroxisomal α-oxidation system, resulting in the accumulation of the branched-chain fatty acid phytanic acid. The main clinical symptoms are polyneuropathy, cerebellar ataxia, and retinitis pigmentosa. To study the pathogenesis of Refsum disease, we generated and characterized a *Phyh* knockout mouse. We studied the pathological effects of phytanic acid accumulation in *Phyh*$^{-/-}$ mice fed a diet supplemented with phytol, the precursor of phytanic acid. Phytanic acid accumulation caused a reduction in body weight, hepatic steatosis, and testicular atrophy with loss of spermatogonia. Phenotype assessment using the SHIRPA protocol and subsequent automated gait analysis using the CatWalk system revealed unsteady gait with strongly reduced paw print area for both fore- and hindpaws and reduced base of support for the hindpaws. Histochemical analyses in the CNS showed astrocytosis and up-regulation of calcium-binding proteins. In addition, a loss of Purkinje cells in the cerebellum was observed. No demyelination was present in the CNS. Motor nerve conduction velocity measurements revealed a peripheral neuropathy. Our results show that, in the mouse, high phytanic acid levels cause a peripheral neuropathy and ataxia with loss of Purkinje cells. These findings provide important insights in the pathophysiology of Refsum disease.

fatty acid oxidation | metabolic disorder | peroxisomes

Refsum disease is an autosomal recessive lipid-storage disorder (MIM266500) characterized by the accumulation of the branched-chain fatty acid phytanic acid (3,7,11,15-tetramethylhexadecanoic acid) in tissues and body fluids of patients (1). Phytanic acid levels are elevated because of a deficiency of the enzyme phytanoyl-CoA hydroxylase (PHYH). PHYH catalyzes the first step of the peroxisomal α-oxidation pathway, i.e., the conversion of phytanoyl-CoA to 2-hydroxy-phytanoyl-CoA. This α-oxidation is required for the degradation of phytanic acid, which contains a methyl group at the third carbon atom of its backbone and therefore cannot be degraded via β-oxidation. As a result of α-oxidation, the terminal carboxyl-group of phytanic acid is released as CO_2, producing pristanic acid, a 2-methyl branched-chain fatty acid (2,6,10,14-tetramethylpentadecanoic acid), which can be degraded via β-oxidation in the peroxisome.

The molecular basis of Refsum disease is heterogeneous, but the majority of patients have mutations in the gene encoding PHYH (2). In humans, the *PHYH* gene is ≈21 kb and consists of 9 exons and 8 introns. It encodes a protein with a calculated mass of 38.6 kDa, including a cleavable peroxisomal targeting signal type 2 (PTS2). This PTS2-signal is recognized by peroxin 7, which is a receptor required for the import of newly synthesized PTS2-containing proteins into peroxisomes. Peroxin 7 is encoded by *PEX7*, which is the second gene that can be mutated in patients with Refsum disease (2). The impaired import of PHYH into the peroxisome leads to a deficient PHYH activity in patients with mutations in the *PEX7* gene.

Clinically, Refsum disease is characterized by cerebellar ataxia, polyneuropathy, and progressive retinitis pigmentosa, culminating in blindness, (1, 3). The age of onset of the symptoms can vary from early childhood to the third or fourth decade of life. No treatment is available for patients with Refsum disease, but they benefit from a low phytanic acid diet. Phytanic acid is derived from dietary sources only, specifically from the chlorophyll component phytol. When phytanic acid levels are kept low via dietary reduction, a halt in the progression of the symptoms has been reported (4–7).

Although the clinical symptoms of Refsum disease are well known, only limited postmortem data are available on Refsum patients and the pathogenesis of the disorder is poorly understood. Insight herein is of crucial importance for the development of potential therapeutic options. Phytanic acid has been claimed to be toxic, and it has been shown to be an activating ligand of the nuclear receptor peroxisome proliferator receptor α (PPARα). To study the pathological consequences of phytanic acid accumulation, we generated of a mouse model for Refsum disease by targeted disruption of the *Phyh* gene.

Results

Disruption of the *Phyh* Gene. To disrupt the mouse *Phyh* gene, part of the gene containing exons 4–7 was replaced with the hygromycin B-resistance gene by homologous recombination in ES cells as depicted in Fig. 1*A*. Correct targeting of *Phyh* was confirmed by Southern blot analysis and PCR on genomic DNA (Fig. 1 *B* and *C*). The disruption of the *Phyh* gene resulted in the absence of detectable mRNA (Fig. 1*D*), PHYH protein, and a complete loss of PHYH enzyme activity (data not shown). The absence of the *Phyh* gene did not result in embryonic lethality nor did it affect postnatal viability. When kept under standard laboratory conditions, *Phyh*$^{-/-}$ mice developed normally and had no obvious developmental abnormalities. They were fertile, and interbreeding of *Phyh*$^{-/-}$ males and females led to viable progeny.

Biochemical Abnormalities in *Phyh*$^{-/-}$ Mice Fed a Phytol-Supplemented Diet. In contrast to the human diet, standard rodent chow contains only low amounts of branched-chain fatty acids and the

Author contributions: S.F., A.W.M.Z., R.J.A.W., P.T.v.d.S., B.T.P.-T., and P.B. designed research; S.F., A.W.M.Z., J.C.K., C.E.v.d.B., M.T., and P.B. performed research; F.P.T.H. contributed new reagents/analytic tools; S.F., A.W.M.Z., J.C.K., and P.B. analyzed data; and S.F., R.J.A.W., P.T.v.d.S., B.T.P.-T., and P.B. wrote the paper.

The authors declare no conflict of interest.

This article is a PNAS Direct Submission.

[1]S.F. and A.W.M.Z. contributed equally to this work.

[2]To whom correspondence should be addressed at: Laboratory Genetic Metabolic Diseases, F0–226, Academic Medical Center, Meibergdreef 9, 1105 AZ Amsterdam, The Netherlands. E-mail: s.ferdinandusse@amc.uva.nl.

This article contains supporting information online at www.pnas.org/cgi/content/full/0806066105/DCSupplemental.

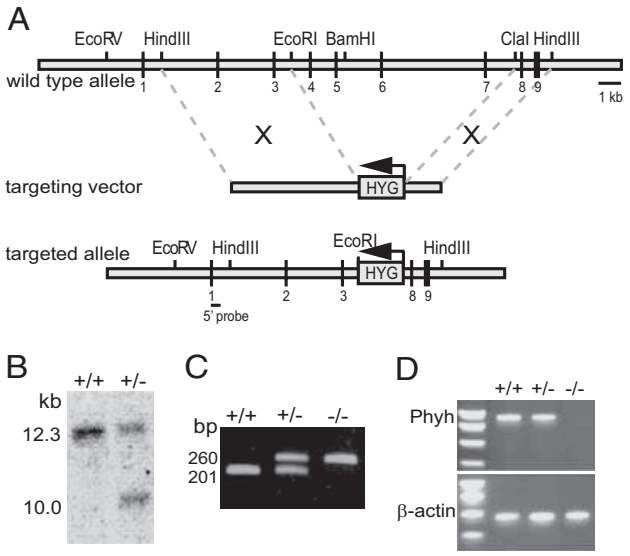

Fig. 1. Generation of targeting vector and *Phyh*$^{-/-}$ mice. (*A*) Strategy of gene targeting. The WT allele, targeting vector and the targeted allele are depicted. After homologous recombination, exons 4–7 and parts of introns 3 and 7 are deleted. The location of the 5′ probe used for Southern blot analysis is shown. (*B*) Southern blot analysis of genomic DNA isolated from ES cells, digested with EcoRV and BamHI, and probed with the 5′ probe yielded a 12.3-kb fragment for the WT allele (+/+) and a 10-kb fragment for the targeted allele (+/−). (*C*) Genotyping by PCR on genomic DNA. Amplification from the WT allele (+/+) resulted in a 201-bp fragment and amplification from the targeted allele (−/−) a fragment of 260 bp. (*D*) (*Upper*) PCR analysis of liver cDNA from WT and *Phyh*$^{-/-}$ mice. No amplification of exons 1–8 could be detected in *Phyh*$^{-/-}$ mice. (*Lower*) A control for cDNA amplification was carried out with primers for β-actin.

phytanic acid precursor phytol. For this reason, we supplemented standard chow with phytol. One group of animals was fed a control diet, 1 group received a diet supplemented with 0.1% (wt/wt) phytol for 6 weeks, and 1 group received a 0.25% (wt/wt) phytol diet for 3 weeks. The 0.25% phytol diet caused a decrease in body weight of 25 ± 5% in the *Phyh*$^{-/-}$ males and 16 ± 10% in the *Phyh*$^{-/-}$ females. This body weight loss is most

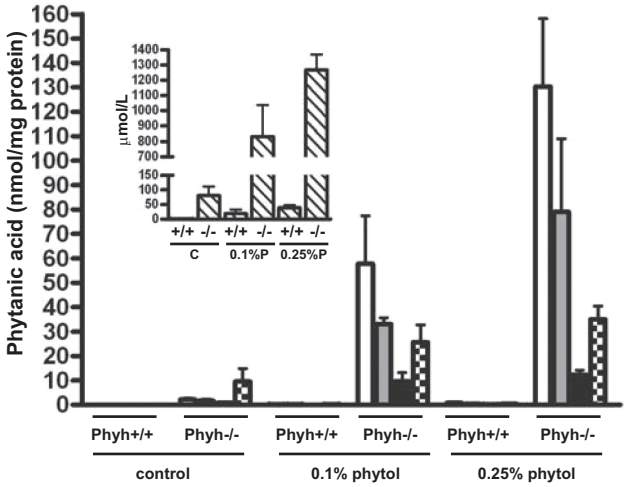

Fig. 2. Phytanic acid levels in plasma and tissues of male WT and *Phyh*$^{-/-}$ mice. Phytanic levels were determined in liver (white bars), kidney (gray bars), cerebellum (black bars), testis (checked bars), and plasma (*Inset* graph) from WT and *Phyh*$^{-/-}$ mice on a control diet (C), a 0.1% phytol diet, and a 0.25% phytol diet. Data represent mean ± SD.

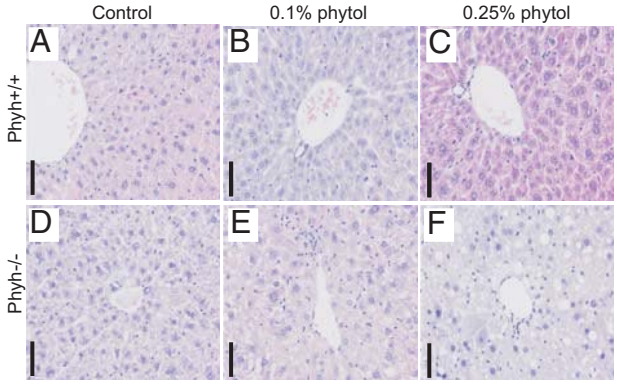

Fig. 3. *Phyh*$^{-/-}$ mice on a phytol diet develop hepatic lipidosis. H&E staining of livers from WT (*A–C*) and *Phyh*$^{-/-}$ mice (*D–F*) on a control diet (*A* and *D*), on a 0.1% phytol diet (*B* and *E*), and on 0.25% phytol diet (*C* and *F*). In *Phyh*$^{-/-}$ mice on a 0.25% phytol diet (*F*), steatosis is clearly detected by the large lipid vacuoles present throughout the liver parenchyma. On a 0.1% phytol diet (*E*), *Phyh*$^{-/-}$ mice showed signs of microsteatosis (small lipid vacuoles within hepatocytes). (Scale bar: 100 μm.)

probably caused by lipoatrophy, because upon dissection, almost no white fat could be observed in the *Phyh*$^{-/-}$ mice after the 0.25% phytol diet.

Because of the phytol diets, phytanic acid accumulated in plasma and tissues (Fig. 2). After 3 weeks on the 0.25% phytol diet, plasma phytanic acid levels >1 mmol/L were reached. Such levels have also been reported in Refsum disease patients (8). Of the different tissues analyzed, liver showed the highest accumulation of phytanic acid, followed by kidney, testis, and cerebellum, and the extent of the accumulation was similar for males and females. These results show that the most important biochemical characteristic of Refsum disease, i.e., phytanic acid accumulation, is reproduced by disruption of the *Phyh* gene in the mouse.

Further biochemical analyses in plasma revealed increased amylase and alanine-amino transferase (ALAT) activity in pooled plasma of *Phyh*$^{-/-}$ mice after 3 weeks on the 0.25% phytol diet, whereas albumin levels were unaltered [supporting information (SI) Table S1]. Cholesterol, triglycerides, free fatty acids, and total fatty acid levels were decreased in plasma from *Phyh*$^{-/-}$ mice on a phytol diet (Table S1). The levels of virtually

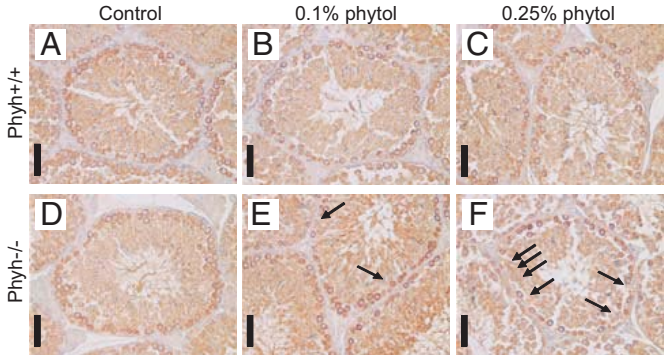

Fig. 4. Loss of spermatogonia in phytol-fed *Phyh*$^{-/-}$ mice. Immunohistochemical detection of calreticulin in testis of WT mice (*A–C*) and *Phyh*$^{-/-}$ (*D–F*) mice on control diet (*A* and *D*), 0.1% phytol diet (*B* and *E*), and 0.25% phytol diet (*C* and *F*). Calreticulin is highly expressed in spermatogonia of WT mice on control diet (*A*). Loss of spermatogonia in *Phyh*$^{-/-}$ mice on the 0.1% phytol (*E*) and 0.25% phytol (*F*) diets is demonstrated by decreased numbers of calreticulin-positive spermatogonia leaving gaps (arrows in *E* and *F*) in the epithelium of the seminiferous tubules. The slide is hematoxylin QS counterstained. (Scale bar: 50 μm.)

BIOCHEMISTRY

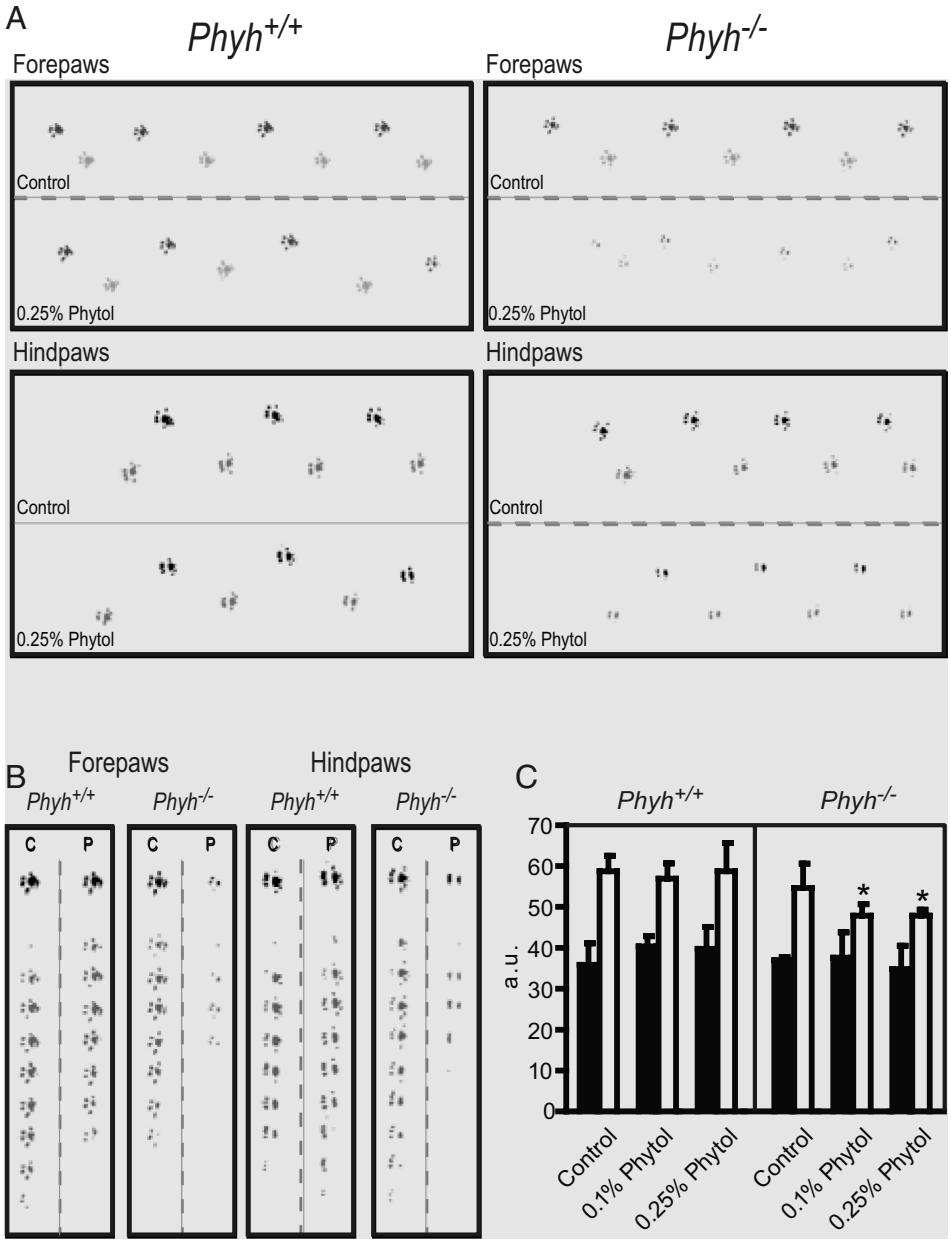

Fig. 5. Automated gait analysis using CatWalk revealed ataxia in *Phyh*$^{-/-}$ mice on a phytol diet. (*A*) Paw prints of the fore- and the hindpaws for representative runs by male WT and *Phyh*$^{-/-}$ mice on different diets are shown. The paw print area of both the fore- and hindpaw of the *Phyh*$^{-/-}$ mice on 0.25% phytol were markedly decreased. (*B*) Successive frames of the paw–floor contact area for fore- and hindpaws revealed a decreased contact area for male *Phyh*$^{-/-}$ mice compared with WT mice on a 0.25% phytol diet. C, control diet; P, 0.25% Phytol diet. (*C*) Base of support for the hindpaws (white bars) was significantly decreased (*, $P < 0.05$, *t* test) in the *Phyh*$^{-/-}$ mice on the phytol diets compared with the base of support of the WT mice on the same diets. The decrease was also significant for the *Phyh*$^{-/-}$ mice before and after the 0.25% phytol diet (data not shown). There were no differences for base of support of the forepaws (black bars).

all of the fatty acids determined were decreased (C14:0, C16:0, C18:0, C20:0, C22:0, and C24:0 and ω3, ω6, ω7, and ω9 polyunsaturated fatty acids). These results confirm that high levels of phytanic acid cause increased fat degradation, resulting in the disappearance of the white fat, as described above.

Pathological Effects of Phytanic Acid Accumulation in *Phyh*$^{-/-}$ Mice. The pathological effects of phytanic acid accumulation in the liver were studied by histological analysis. H&E staining of liver sections (Fig. 3) of *Phyh*$^{-/-}$ mice fed with the 0.25% phytol diet showed morphological changes that included steatosis, hepatocyte degeneration, and inflammatory infiltrates. The steatosis in livers from *Phyh*$^{-/-}$ mice was microvesicular when they were fed the 0.1% phytol diet (Fig. 3*E*) and macrovesicular when fed the 0.25% phytol diet (Fig. 3*F*). In contrast, no morphological changes were observed in WT mice when fed a phytol diet.

H&E staining of testis sections revealed that, despite having sperm at different stages of maturation, the seminiferous tubules of *Phyh*$^{-/-}$ mice on the phytol diet did not have the full complement of spermatogenic cells (Fig. 4). This loss of spermatogenic cells was clearly seen upon immunodetection of calreticulin, which is predominantly expressed in spermatogonia. After 6 weeks on the 0.1% phytol diet, loss of spermatogonia was clearly visible (Fig. 4*E*), but mild when compared with the loss observed after 3 weeks on the 0.25% phytol diet (Fig. 4*F*). No abnormalities were observed by histological analysis in heart, kidney, intestine, lung and eye.

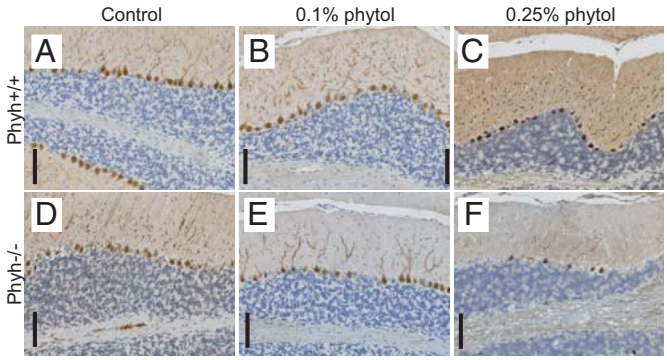

Fig. 6. Loss of Purkinje cells in the cerebellum of *Phyh*$^{-/-}$ mice fed phytol. Immunohistochemical detection of calbindin-D28K in the cerebellum of WT (*A–C*) and *Phyh*$^{-/-}$ (*D–F*) mice fed a control diet (*A* and *D*), a 0.1% phytol diet (*B* and *E*), and a 0.25% phytol diet (*C* and *F*). Small areas lacking Purkinje cells are evident in the cerebellum of *Phyh*$^{-/-}$ mice fed the 0.1% phytol diet (*E*). Widespread loss of Purkinje cells is observed in the cerebellum of *Phyh*$^{-/-}$ mice fed the 0.25% phytol diet, with only a few surviving Purkinje cells (*F*). The slide is hematoxylin QS counterstained. (Scale bar: 100 μm.)

Phenotype Assessment—Behavioral Tests. To assess the phenotype of the *Phyh*$^{-/-}$ mice, we used the SHIRPA protocol as primary screen (9). Twenty-four tests were performed with all of the mice before and after the diet period. *Phyh*$^{-/-}$ mice after the phytol diet had a deviating score for some tests, pointing to abnormalities in neuromuscular function. Both male and female *Phyh*$^{-/-}$ mice showed an increased number of paw slips while moving on a grid. Trunk curl was absent in *Phyh*$^{-/-}$ males after the phytol diets, whereas it was present in the mice before the diets. In addition, the gait of both male and female *Phyh*$^{-/-}$ mice after the phytol diets was scored fluid but abnormal, whereas their gait was normal before the diet. The gait of the WT mice was normal regardless of their diet.

Automated Quantitative Gait Analysis. Because the SHIRPA protocol revealed gait abnormalities, locomotion was subsequently analyzed in more detail by using CatWalk automated gait analysis (10). *Phyh*$^{-/-}$ mice developed an abnormal gait because of the phytol diet, and the abnormalities were most striking in animals fed with a 0.25% phytol diet. As seen in Fig. 5*A*, the paw print area (the total area of the paw contacting the floor during stance phase) of both fore- and hindpaws was decreased in *Phyh*$^{-/-}$ mice on the 0.25% phytol diet. In addition, the spread of the intermediate toes of the hindpaws was decreased. The analysis of the successive frames of the paw–floor contact area for individual fore- and hindpaws, clearly showed decreased contact areas for *Phyh*$^{-/-}$ mice compared with WT mice on the 0.25% phytol diet (Fig. 5*B*). At the same time, the duration of the stance phase did not differ significantly between the different groups (data not shown). The base of support (average distance between the mass midpoints of the prints at maximum contact) of the hindpaws for male *Phyh*$^{-/-}$ mice decreased because of the phytol diet (Fig. 5*C*). There was no correlation between the base of support and weight of the animals at the time of the CatWalk analysis. No differences were found in the base of support of the forepaws for both *Phyh*$^{-/-}$ males and females. The gait abnormalities observed in *Phyh*$^{-/-}$ mice point to a neuropathy induced by phytanic acid accumulation.

CNS Abnormalities in *Phyh*$^{-/-}$ Mice. To determine potential CNS pathology, we performed macro- and microscopic analyses of brain and spinal cord. No gross abnormalities were observed in brains of *Phyh*$^{-/-}$ mice upon dissection. Immunostaining with an antibody against myelin basic protein (MBP) revealed normal myelination in the cerebral cortex and spinal cord of *Phyh*$^{-/-}$ mice regardless of the dietary regimen (data not shown). However, glial fibrillary acidic protein (GFAP) immunohistochemistry (Fig. S1) revealed reactive astrocytosis in the brain of *Phyh*$^{-/-}$ mice fed with the 0.25% phytol diet. Astrocytosis was prominent in the inferior colliculus (Fig. S1*F*) and thalamus (data not shown). Occasionally, reactive astrocytes were identified in the granular layer of the cerebellum (Fig. S1*J*), but normal appearing astrocytes were present in the hippocampus (Fig. S1*K*) and spinal cord (Fig. S1*L*). Calbindin-D28K immunohistochemistry (Fig. 6) and quantification of Purkinje cells revealed a decrease in Purkinje cell numbers in *Phyh*$^{-/-}$ mice fed phytol (Fig. S2). When *Phyh*$^{-/-}$ mice were fed with the 0.1% phytol diet, we observed focal loss of Purkinje cells within the cerebellar Purkinje cell layer (Fig. 6*E*). A severe loss of Purkinje cells with only some remaining foci of surviving Purkinje cells (Fig. 6*F*), that showed an abnormal truncated arborization, was observed after the 0.25% phytol diet. Within the cerebrum, an increase in the number of calbindin-D28K-positive neurons was observed in the cortex, thalamus, and medulla of *Phyh*$^{-/-}$ mice fed with the 0.25% phytol diet (data not shown). This observation led us to investigate the expression of calcium-binding proteins in the CNS. Parvalbumin expression was clearly increased in the thalamus and cerebral cortex of *Phyh*$^{-/-}$ mice with the highest expression after the 0.25% phytol diet (Fig. S3). The number of cortical neurons expressing parvalbumin was also increased in *Phyh*$^{-/-}$ mice fed the phytol diets (Fig. S3). Expression of calreticulin in the CNS was similar between WT and *Phyh*$^{-/-}$ mice regardless of the dietary regimen (data not shown). In conclusion, our immunohistochemical analyses have shown that phytanic acid accumulation causes pathological and adaptive changes in the CNS of *Phyh*$^{-/-}$ mice.

Peripheral Neuropathy in *Phyh*$^{--}$ mice. To determine whether a peripheral neuropathy is present in *Phyh*$^{-/-}$ mice, motor nerve conduction velocities (MNCV) were measured. The measurements revealed a significant decrease in MNCV in *Phyh*$^{-/-}$ mice fed with a 0.1% phytol diet for 8 weeks (Fig. S4). The MNCV in *Phyh*$^{-/-}$ mice after the phytol diet was 22.7 $\pm$ 3.2 m/s compared with 29.6 $\pm$ 0.6 m/s in WT mice. This decrease in MNCV was due to an increased latency in the compound muscle action potentials after stimulation (Fig. S4). The action potentials were also extended in *Phyh*$^{-/-}$ mice. On the control diet, *Phyh*$^{-/-}$ mice had normal MNCV with normal compound muscle action potentials. These results show that the phytol diet causes a peripheral neuropathy in *Phyh*$^{-/-}$ mice. Histological analyses and MBP immunohistochemistry of sciatic nerves from WT and *Phyh*$^{-/-}$ mice did not reveal gross abnormalities in myelination (Fig. S4).

Discussion

Only limited postmortem data are available on Refsum patients, and the pathophysiology of Refsum disease is poorly understood. In this article, we report studies on the pathological consequences of phytanic acid accumulation in a *Phyh*$^{-/-}$ mouse, which we generated as model for the human disorder. Because phytanic acid is present in numerous dietary sources, Refsum patients are life-long exposed to elevated phytanic acid levels. During metabolic stress due to fasting or a viral infection, stored phytanic acid is mobilized from adipose tissue, causing a rapid rise of plasma phytanic acid levels, thus accelerating the progression of clinical symptoms (1, 3). The *Phyh*$^{-/-}$ mice in this study received a phytol-supplemented diet for a relatively short period (up to 6 weeks), allowing us to study the short-term effect of phytanic acid accumulation. The plasma phytanic acid levels that were reached in the *Phyh*$^{-/-}$mice were similar to those found in plasma from Refsum patients (8). We observed several detrimental effects caused by the high phytanic acid levels. First of all, *Phyh*$^{-/-}$ mice displayed a severe weight loss on the diet

with the highest phytol concentration. This was accompanied by lipoatrophy and hepatic lipidosis. At the same time, plasma levels of triglycerides, cholesterol, and fatty acids were decreased. These changes are most likely due to activation of peroxisome proliferator receptor α (PPARα) by phytanic acid. Phytanic acid has been shown to be an activating ligand of this nuclear receptor (11–13), which regulates the expression of genes involved in lipid and lipoprotein metabolism and fatty acid oxidation both in humans and rodents (14–16). The expression of peroxisomal straight-chain acyl-CoA oxidase, a target gene of PPARα (14), was up-regulated in *Phyh*$^{-/-}$ mice on a phytol diet (data not shown) pointing to PPARα activation in these mice. Indeed, *Phyh:PPAR*α double-knockout mice fed for 3 weeks with a 0.25% phytol diet did not lose any weight, confirming the involvement of PPARα in the phytanic acid induced weight loss in *Phyh*$^{-/-}$ mice (data not shown).

Toxicity of high phytanic acid levels could be observed in different tissues of the *Phyh*$^{-/-}$ mice. In the liver of *Phyh*$^{-/-}$ mice, the 0.25% phytol diet caused not only steatosis but also hepatocyte degeneration and infiltration. Phytol treatment also resulted in increased plasma levels of ALAT and amylase, indicative of liver and pancreas damage. In addition, a loss of spermatogonia was observed in the testis of phytol-fed *Phyh*$^{-/-}$ mice. Longer exposure to these high levels of phytanic acid may lead to a block in spermatogenesis, which has been described for Refsum patients (17).

Phenotype assessment with the SHIRPA protocol and subsequent automated gait analysis using the CatWalk system revealed an abnormal gait for *Phyh*$^{-/-}$ mice on the phytol diet. The toe spread, paw print area, and base of support of the hindpaws were all decreased, leading to an unsteady gait. The decreased toe spread is indicative of denervation of intrinsic foot muscles (18) and a peripheral neuropathy as shown by decreased MNCV. The neuropathy in *Phyh*$^{-/-}$ mice resembles the axonopathy shown in several Refsum patients (19, 20), characterized by marginal decreases in MNCV and no gross demyelination. The abnormal paw print with decreased paw print area is suggestive of pedes cavi, which is a clinical feature of Refsum disease (21) and other peripheral neuropathies like Charcot–Marie–Tooth disease. Interestingly, histochemical analysis in the cerebellum revealed a loss of Purkinje cells, which is known to cause cerebellar ataxia (22), a prominent feature in Refsum disease (1, 3). A role of phytanic acid in the death of Purkinje cells has been suggested in rhizomelic chondrodysplasia punctata type I (23), another peroxisomal disorder associated with phytanic acid accumulation. Astrocytosis in the inferior colliculus, thalamus, and cerebellum was an additional remarkable consequence of phytanic acid accumulation in the CNS.

We observed a striking up-regulation of the calcium-binding proteins calbindin and parvalbumin in the cerebral cortex, thalamus, and medulla of *Phyh*$^{-/-}$ mice due to the phytanic acid accumulation. In vitro studies have shown that rat hippocampal astrocytes show an increase of cytosolic calcium due to activation of intracellular calcium stores in response to exposure to phytanic acid (24–26). This suggests that the up-regulation of the calcium-binding proteins could be a neuroprotective mechanism to protect against excitotoxicity caused by phytanic acid.

In conclusion, our studies have provided important insights in the pathophysiology of Refsum disease. As a consequence of phytanic acid accumulation, *Phyh*$^{-/-}$ mice, just like human patients, developed a peripheral neuropathy and cerebellar ataxia that was accompanied by a loss of Purkinje cells. In addition, the increased phytanic acid levels caused reactive astrocytosis, and up-regulation of the calcium-binding proteins in the CNS, which is most likely a neuroprotective mechanism against the excitotoxic effects of phytanic acid. Our studies showed that *Phyh*$^{-/-}$ mice are a good model for this human disorder. Future studies will focus on the effects of long-term exposure to high levels of phytanic acid. Studies in *Phyh*$^{-/-}$ mice will be valuable for the development and evaluation of potential new treatment options.

Materials and Methods

Construction of the Targeting Vector and Generation of *Phyh*$^{-/-}$ Mice. The *Phyh* gene (GenBank accession no. NP_034856.1) was cloned from a 129 SVJ mouse genomic library (Stratagene). The targeting vector was constructed by removing an EcoRI-ClaI fragment including exons 4–7 and replacing it with the hygromycin B resistance gene in the opposite transcriptional orientation to the *Phyh* gene. The final construct contained 6.3 kb and 2 kb of 5′ and 3′ homology, respectively. The targeting vector (30 μg) was linearized with HindIII and introduced into IB10 ES cells (The Netherlands Cancer Institute, 6×10^6cells) by electroporation (0.8 kV and 3 μF) in a Bio-Rad gene pulser. Targeted ES cells were screened by PCR for homologous recombination. The primers annealed to the hygromycin B resistance marker and the 3′ genomic flank outside the construct, respectively. PCR positive clones were also analyzed by Southern blot for correct 5′ homologous recombination. Genomic DNA was digested overnight with EcoRV and BamHI and hybridization of the Southern blot was carried out with an external 5′ probe (EcoRI-HincII fragment, containing exon 1). Targeted ES cells were injected in C57BL/6 blastocysts, resulting in several chimeric mice that showed germ-line transmission. *Phyh*$^{+/-}$ mice (50%Swiss/25%129SVJ/25%FVB) were crossbred to obtain *Phyh*$^{+/+}$ and *Phyh*$^{-/-}$ animals. F2 offspring were used for the experiments. Mice were genotyped by PCR analysis on genomic DNA. The sequence of the forward primer for the WT allele was 5′-CTC TCC AAT CTT AGT CGG TC-3′ (located in intron 7) and the sequence of the forward primer for the targeted allele was 5′-CTA CCG GTG GAT GTG GAA TG-3′ (located in the promoter of the hygromycin B resistance gene). One reverse primer was used with both forward primers: 5′-CCC TAG CGT TTC CTC TGT G-3′ (located in intron 8) at an annealing temperature of 55 °C. The PCR product obtained from amplification of the WT allele was 201 bp and 260 bp for the targeted allele.

Animal Experiments. Seven-week-old WT and *Phyh*$^{-/-}$ mice were fed pelleted mouse chow (AB Diets) without supplements (control) or supplemented with 0.1% (wt/wt) phytol or 0.25% (wt/wt) phytol (Sigma–Aldrich). Each group consisted of 6 animals, including 3 males and 3 females that were 7 weeks old at the start of the experiment. The mice received the diet for 3 weeks in the case of the 0.25% phytol diet and for 6 weeks in the case of the control and 0.1% phytol diet. At the start and at the end of the diet period, the SHIRPA protocol was performed with all animals, and the gait was analyzed by using CatWalk. At the end of the experiment, mice were anesthetized by using isoflurane, blood was collected by cardiac puncture, and tissues were harvested. The animals were killed the day after the final SHIRPA and CatWalk analysis, and they had free access to water and food until that moment. Tissues were snap-frozen in liquid nitrogen and stored at −80 °C for further analysis. For the MNCV measurements, another set of animals was used. For these measurements, WT and *Phyh*$^{-/-}$ mice were fed a control or a 0.1% (wt/wt) phytol supplemented diet for 8 weeks. All animal experiments were approved by the University of Amsterdam Animals Experiments Committee.

Biochemical Analyses. Phytanic acid levels were determined by gas-chromatography mass spectrometry as described (27). Very long-chain, straight-chain, mono-, and polyunsaturated fatty acids were analyzed by capillary gas chromatography (28, 29). Amylase, ALAT, free fatty acids, cholesterol, and triglycerides were measured according to standard procedures in the Institut Clinique de la Souris (Strasbourg, France).

SHIRPA Protocol. A total of 24 separate measurements of the SHIRPA protocol (9) were recorded for each animal at the beginning and at the end of the diet period. Assessment of each animal began with observation of undisturbed behavior in a cylindrical clear perspex viewing jar. The mice were then transferred to an arena for observation of motor behavior. This was followed by a sequence of manipulations using tail suspension, where measurements of visual acuity, grip strength, body tone, and reflexes were recorded. Subsequently, negative geotaxis and contact righting reflex were measured, and a wire maneuver was performed. Finally, the animal was restrained in supine position to measure limb tone.

CatWalk Automated Quantitative Gait Analysis. The gait of the mice was analyzed by using the CatWalk program (10). This program acquires data when mice are filmed with a CCD camera from below while traversing a walkway with a glass floor in a dark room. Alongside the long edge of the glass light enters the glass, which is reflected by paws placed on the walkway. The

animals were allowed to traverse the walkway as many times as needed to obtain at least 3 fluent crossings (without stopping or hesitations). Both qualitative and quantitative data can be assessed with the CatWalk program. For this study, we focused on the paw print, the paw print area, and the base of support (average distance between the mass-midpoints of the prints at maximum contact).

Histological and Immunohistochemical Analyses. Harvested tissues were fixed by immersion in formalin at 4 °C for 48 h and processed for paraffin embedding. For immunohistochemistry, 5-μm sections were cut on a Leica RM2255 microtome and stained with H&E for microscopic pathologic analyses. For immunohistochemistry, sections were cleared in Histoclear II (National Diagnostics), hydrated to water in graded alcohol series, and processed for DAB-immunostaining following a standard protocol using Vectorstain Elite ABC kit (Vector Laboratories) for polyclonal antibodies and the Vector M.O.M. kit (Vector Laboratories) for mouse monoclonals and visualized by using DAB (Sigma). Sections were counterstained with hematoxylin QS (Vector Laboratories), dehydrated in graded alcohol series, cleared in Histoclear II, and mounted with DPX (Fluka). Sections were analyzed in a Zeiss Axiophot microscope equipped with a Leica DFC320 camera. Primary antibodies used in this study were, against GFAP (rabbit polyclonal; DAKO Cytomation), MBP (goat polyclonal, C16; Santa Cruz Biotechnology), calbindin-D28K (Mouse monoclonal, clone CB955; Sigma–Aldrich), parvalbumin (mouse monoclonal, clone Parv19; Sigma–Aldrich), calreticulin (goat polyclonal, C17; Santa Cruz Biotechnology). For the calculation of the numbers of calbindin-D28K-positive Purkinje cells and parvalbumin-positive cortical neurons, 3 nonadjacent sections (separated by 250 μm) from the midline were analyzed. Purkinje cells were counted in entire cerebellar slices. Parvalbumin-positive neurons were counted in a 0.1-mm^2 area comprising the motor and visual cortex.

MNCV Measurements. Mice were anesthetized with ketamine and xylazine (100 mg/kg and 10 mg/kg, respectively). Recording needle electrodes were placed in the foot pad, and supramaximal stimulation of sciatic nerves was performed distally at the ankle and proximally at the sciatic notch. Recordings were obtained on a PowerLab 4/25T (AD Instruments) using Chart5 software. Conduction velocities were calculated as (proximal distance − distal distance)/(proximal latency − distal latency), with latencies corresponding to the time lapse between the stimulus and the onset of the compound muscle action potential and expressed in meters per second.

ACKNOWLEDGMENTS. We thank the Institut Clinique de la Souris, (Strasbourg, France) for the measurement of the clinical chemical parameters; the people at the animal facility at the Academic Medical Center and the Hubrecht Institute and D. M. van den Brink, H. Rusch, and A. van Cruchten for technical assistance; and H. R. Waterham and S. M. Houten for helpful discussion and critical reading of the manuscript. This work was supported by the Prinses Beatrix Fund Grant Mar 04-0116, by Association Européenne Contre les Leucodystrophies Grant 2005-017I4, and by European Union Grants QLG3-CT-2002-00696 (''Refsum's disease: Diagnosis, pathology, and treatment'') and LSHG-CT-2004-512018 (''Peroxisomes in health and disease'').

1. Wanders RJA, Jakobs C, Skjeldal OH (2001) in *The Molecular and Metabolic Bases of Disease*, eds Scriver CR, Beaudet AL., Sly WS, Valle D (McGraw–Hill, New York), pp 3303–3321.
2. Jansen GA, Waterham HR, Wanders RJ (2004) Molecular basis of Refsum disease: Sequence variations in phytanoyl-CoA hydroxylase (PHYH) and the PTS2 receptor (PEX7). *Hum Mutat* 23:209–218.
3. Wierzbicki AS, *et al.* (2002) Refsum's disease: A peroxisomal disorder affecting phytanic acid alpha-oxidation. *J Neurochem* 80:727–735.
4. Eldjarn L, *et al.* (1966) Dietary effects on serum-phytanic-acid levels and on clinical manifestations in heredopathia atactica polyneuritiformis. *Lancet* 287:691–693.
5. Gibberd FB, Billimoria JD, Page NG, Retsas S (1979) Heredopathia atactica polyneuritiformis (Refsum's disease) treated by diet and plasma-exchange. *Lancet* 313:575–578.
6. Hungerbuhler JP, *et al.* (1985) Refsum's disease: Management by diet and plasmapheresis. *Eur Neurol* 24:153–159.
7. Masters-Thomas A, *et al.* (1980) Heredopathia atactica polyneuritiformis (Refsum's disease): 1. Clinical features and dietary management. *J Hum Nutr* 34:245–250.
8. Wierzbicki AS, *et al.* (2003) Metabolism of phytanic acid and 3-methyl-adipic acid excretion in patients with adult Refsum disease. *J Lipid Res* 44:1481–1488.
9. Rogers DC, *et al.* (1997) Behavioral and functional analysis of mouse phenotype: SHIRPA, a proposed protocol for comprehensive phenotype assessment. *Mamm Genome* 8:711–713.
10. Hamers FP, *et al.* (2001) Automated quantitative gait analysis during overground locomotion in the rat: Its application to spinal cord contusion and transection injuries. *J Neurotrauma* 18:187–201.
11. Gloerich J, *et al.* (2005) A phytol-enriched diet induces changes in fatty acid metabolism in mice both via PPARalpha-dependent and -independent pathways. *J Lipid Res* 46:716–726.
12. Heim M, *et al.* (2002) Phytanic acid, a natural peroxisome proliferator-activated receptor (PPAR) agonist, regulates glucose metabolism in rat primary hepatocytes. *FASEB J* 16:718–720.
13. Zomer AW, *et al.* (2000) Pristanic acid and phytanic acid. Naturally occurring ligands for the nuclear receptor peroxisome proliferator-activated receptor alpha. *J Lipid Res* 41:1801–1807.
14. Aoyama T, *et al.* (1998) Altered constitutive expression of fatty acid-metabolizing enzymes in mice lacking the peroxisome proliferator-activated receptor alpha (PPARalpha). *J Biol Chem* 273:5678–5684.
15. Peters JM, *et al.* (1997) Alterations in lipoprotein metabolism in peroxisome proliferator-activated receptor alpha-deficient mice. *J Biol Chem* 272:27307–27312.
16. Duval C, Muller M, Kersten S (2007) PPARalpha and dyslipidemia. *Biochim Biophys Acta* 1771:961–971.
17. Cammermeyer J (1975) in *Handbook of Clinical Neurology*, eds Vinken PJ, Bruyn GW (North–Holland, Amsterdam), pp 231–261.
18. Inserra MM, Bloch DA, Terris DJ (1998) Functional indices for sciatic, peroneal, and posterior tibial nerve lesions in the mouse. *Microsurgery* 18:119–124.
19. Gelot A, Vallat JM, Tabaraud F, Rocchiccioli F (1995) Axonal neuropathy and late detection of Refsum's disease. *Muscle Nerve* 18:667–670.
20. Salisachs P (1982) Ataxia and other data reviewed in Charcot–Marie–Tooth and Refsum's disease. *J Neurol Neurosurg Psychiatry* 45:1085–1091.
21. Wills AJ, Manning NJ, Reilly MM (2001) Refsum's disease. *Q J Med* 94:403–406.
22. Lalonde R, Strazielle C (2007) Spontaneous and induced mouse mutations with cerebellar dysfunctions: Behavior and neurochemistry. *Brain Res* 1140:51–74.
23. Powers JM, Kenjarski TP, Moser AB, Moser HW (1999) Cerebellar atrophy in chronic rhizomelic chondrodysplasia punctata: A potential role for phytanic acid and calcium in the death of its Purkinje cells. *Acta Neuropathol* 98:129–134.
24. Kahlert S, Schonfeld P, Reiser G (2005) The Refsum disease marker phytanic acid, a branched chain fatty acid, affects Ca2+ homeostasis and mitochondria, and reduces cell viability in rat hippocampal astrocytes. *Neurobiol Dis* 18:110–118.
25. Reiser G, Schonfeld P, Kahlert S (2006) Mechanism of toxicity of the branched-chain fatty acid phytanic acid, a marker of Refsum disease, in astrocytes involves mitochondrial impairment. *Int J Dev Neurosci* 24:113–122.
26. Schonfeld P, Kahlert S, Reiser G (2006) A study of the cytotoxicity of branched-chain phytanic acid with mitochondria and rat brain astrocytes. *Exp Gerontol* 41:688–696.
27. Vreken P, *et al.* (1998) Rapid stable isotope dilution analysis of very-long-chain fatty acids, pristanic acid and phytanic acid using gas chromatography-electron impact mass spectrometry. *J Chromatogr B* 713:281–287.
28. Dacremont G, Cocquyt G, Vincent G (1995) Measurement of very long-chain fatty acids, phytanic and pristanic acid in plasma and cultured fibroblasts by gas chromatography. *J Inherit Metab Dis* 18 Suppl 1:76–83.
29. Dacremont G, Vincent G (1995) Assay of plasmalogens and polyunsaturated fatty acids (PUFA) in erythrocytes and fibroblasts. *J Inherit Metab Dis* 18:84–89.